Development 140, 3486-3495 (2013) doi:10.1242/dev.094011

The NM23-H1/H2 homolog NDK-1 is required for full activation of Ras signaling in *C. elegans*

Neda Masoudi[1,2,*], Luca Fancsalszky[1,*], Ehsan Pourkarimi[1,2,*], Tibor Vellai[1], Anita Alexa[3,4], Attila Reményi[3,4], Anton Gartner[2], Anil Mehta[5] and Krisztina Takács-Vellai[1,‡]

SUMMARY

The group I members of the Nm23 (non-metastatic) gene family encode nucleoside diphosphate kinases (NDPKs) that have been implicated in the regulation of cell migration, proliferation and differentiation. Despite their developmental and medical significance, the molecular functions of these NDPKs remain ill defined. To minimize confounding effects of functional compensation between closely related Nm23 family members, we studied *ndk-1*, the sole *Caenorhabditis elegans* ortholog of group I NDPKs, and focused on its role in Ras/mitogen-activated protein kinase (MAPK)-mediated signaling events during development. *ndk-1* inactivation leads to a protruding vulva phenotype and affects vulval cell fate specification through the Ras/MAPK cascade. *ndk-1* mutant worms show severe reduction of activated, diphosphorylated MAPK in somatic tissues, indicative of compromised Ras/MAPK signaling. A genetic epistasis analysis using the vulval induction system revealed that NDK-1 acts downstream of LIN-45/Raf, but upstream of MPK-1/MAPK, at the level of the kinase suppressors of ras (KSR-1/2). KSR proteins act as scaffolds facilitating Ras signaling events by tethering signaling components, and we suggest that NDK-1 modulates KSR activity through direct physical interaction. Our study reveals that *C. elegans* NDK-1/Nm23 influences differentiation by enhancing the level of Ras/MAPK signaling. These results might help to better understand how dysregulated Nm23 in humans contributes to tumorigenesis.

KEY WORDS: *C. elegans*, KSR scaffolds, Nm23/NDPK, NME, Ras signaling

INTRODUCTION

The human NME family (legacy nomenclature Nm23) consists of ten proteins, which are classified into two groups based on their sequence homology and nucleoside diphosphate kinase (NDPK) activity (Desvignes et al., 2009). Four members belonging to group I (NM23-H1 to -H4, now known as NME1-4) show high sequence similarity and a NDPK activity: group I NDPKs transfer phosphate to cognate dinucleotides through a highly conserved phosphohistidine intermediate (Steeg et al., 2003). The group II proteins of the Nm23 family (NM23-H5 to -H10, now known as NME5-9 and RP2) are more divergent and not necessarily active kinases. A group I NDPK, NM23-H1, was the first identified metastasis inhibitor (Steeg et al., 1988), with reduced levels or absence primarily detected in breast cancer (Heimann and Hellman, 2000). However, NM23-H1 was found to be overexpressed in ovarian, prostate and pancreatic cancers, suggesting a prominent, contributing role in tumor development (Harłozińska et al., 1996; Igawa et al., 1994; Andolfo et al., 2011; Takadate et al., 2012). Despite its significance in tumorigenesis, little is known about the developmental roles of NM23-H1. In *Drosophila*, deletion of the sole fly group I NDPK homolog *abnormal wing discs* (*awd*) induces imaginal disc cell death during larval development (Biggs et al., 1990). Mutations in *awd* also disrupt epithelial tubule morphogenesis during fly tracheal embryogenesis (Dammai et al., 2003).

Nucleoside diphosphates might not be the sole recipients of the high-energy phosphate transferred from H118 (histidine 118 residue) in group I members. In mammalian cells, NM23-H2 (NME2) can relay its high-energy phosphate to histidines located in various target proteins. For example, histidine phosphorylation of the beta subunit of heterotrimeric G proteins by NDPK-H2 augments cyclic AMP formation in the heart (Hippe et al., 2009) and phosphohistidine modification of the ATP-citrate lyase by NM23-H1 (NME1) is needed for its enzymatic activity (Wagner and Vu, 1995).

Besides the above-described biochemical and developmental activities, NDPKs have also been considered to act as, or to modify the activity of other, scaffold proteins. Recently, evidence was presented that NDPK-H2 is required as a scaffold that links heterotrimeric G proteins to caveolins (Hippe et al., 2011). Apparently, this complex regulates G protein content at the plasma membrane, thereby influencing cardiac contractility. NDPKs can locally enrich GTP and thus may control endocytosis through the function of the GTPase dynamin (Dammai et al., 2003) and small G proteins such as Rac (Rochdi et al., 2004). Furthermore, based on studies on human cell lines, NM23-H1 has been suggested to interact with the kinase suppressor of ras 1 (KSR1) scaffold protein (Hartsough et al., 2002; Salerno et al., 2005). In cell lines, phosphorylation of KSR1 by NM23-H1 leads to attenuation of Ras/ERK signaling (Hartsough et al., 2002). These diverse molecular functions of NDPKs might explain the documented pleiotropic effects of NDPK overexpression or deletion across species. There are also examples of important roles for NDPK in cell migration, growth and differentiation (Lee et al., 2009; Mochizuki et al., 2009), which might explain why NDPKs have

[1]Department of Genetics, Eötvös Loránd University, Pázmány Péter stny. 1/C, H-1117 Budapest, Hungary. [2]Wellcome Trust Centre for Gene Regulation and Expression, University of Dundee, Dow Street, Dundee DD1 5EH, UK. [3]Department of Biochemistry, Eötvös Loránd University, Pázmány Péter stny. 1/C, H-1117 Budapest, Hungary. [4]Institute of Molecular Pharmacology, Research Centre for Natural Sciences, Hungarian Academy of Sciences, Pusztaszeri út 59-67, H-1025 Budapest, Hungary. [5]Division of Medical Sciences, Centre for CVS and Lung Biology, Ninewells Hospital Medical School, Dundee DD1 9SY, UK.

*These authors contributed equally to this work
‡Author for correspondence (takacsve@gmail.com)

Accepted 17 June 2013

been repeatedly implicated in various cancers while also appearing to act in apparently unrelated signaling processes.

To understand the mechanisms underpinning such diverse functions, we used the nematode *Caenorhabditis elegans* as a tractable genetic model whose genome encodes only a single mammalian group I NDPK ortholog (Bilitou et al., 2009), which we named NDK-1 (nucleoside diphosphate kinase-1). To pin down the function of NDK-1, we focused on the vulva and studied defects associated with the morphogenesis of this organ in nematodes defective for NDK-1. In addition, we used the well-characterized vulva induction system to place NDK-1 function into Ras/MAPK signaling. The vulva of the *C. elegans* hermaphrodite develops from a subset of six multipotent epidermal cells called vulval precursor cells (VPCs), consecutively termed P3.p to P8.p (Sternberg, 2005). An inductive signal conferred by an epidermal growth factor (EGF) ligand expressed from the gonadal anchor cell (AC) activates the Ras/MAPK pathway in P(5-7).p cells, causing them to adopt specific vulval cell fates. P6.p, the VPC closest to the AC, adopts the primary vulval fate, while P5.p and P7.p, the two adjacent VPCs to P6.p, adopt the secondary vulval fate as a result of lateral signaling, which is mediated by the LIN-12/Notch pathway (Greenwald, 2005). By contrast, P3.p, P4.p and P8.p, the VPCs farthest from the AC, receive only a basal level of Ras activation, thereby expressing the non-induced tertiary fate. Constitutive activation of the Ras/MAPK pathway leads to ectopic induction of the primary and secondary fate in the latter cells (P3.p, P4.p and P8.p), resulting in a multivulva (Muv) phenotype. Conversely, lack of Ras signaling causes a vulvaless (Vul) phenotype (none of the VPCs adopts an induced vulval fate).

In this study, we report that *ndk-1* is an essential gene. Moreover, *ndk-1* loss-of-function mutants show defects in the morphogenesis of the vulva. We demonstrate that NDK-1 augments – rather than attenuates, as in the case of human cell lines – the extent of Ras/MAPK signaling. We find that the extent of Ras/MAPK-dependent vulva induction is reduced in *ndk-1* mutants, and that NDK-1 enhances Ras/MAPK signaling downstream of Raf at the level of the KSR scaffold proteins, probably through direct physical interaction. We also provide evidence that NDK-1 affects further developmental and physiological events that rely on Ras/MAPK signaling.

MATERIALS AND METHODS

Nematode strains and alleles

The wild-type *C. elegans* strain corresponds to var. Bristol (N2). The following mutant strains were used: EJ810 *F25H2.5(ok314)/hT2[dpy-18(h662)]I; +/hT2[bli-4(e937)]III*; TTV1 *ndk-1(ok314) I/hT2[bli-4(e937) let-?(q782) qIs48](I;III)*; UP749 *ksr-2(dx27)I/hT2[bli-4(e937) let-?(q782) qIs48](I;III)*; BC12969 *dpy-5(e907)I; sIs12774[rCesF52H2.5::GFP + pCeh361]*; TTV4 *ksr-2(dx27)ndk-1(ok314)/hT2[bli-4(e937) let-?(q782) qIs48](I;III)*, TTV2 *eluEx1[NDK-1::gfp; unc-119(+)];unc-119(ed3)III*; TTV3 *eluSi1*[NDK-1::GFP + *cb-unc-119(+)*]*III*; PS1839 *let-23(sa62)II*; MT2131 *lin-31(n1053)II*; MT2124 *let-60(n1046)IV*; MT4698 *let-60(n1700)IV*; CB1275 *lin-1(e1275)IV*; NH2466 *ayIs4 (egl-17::gfp)I; dpy-20(e1282)IV;* kuIs57 *col-10::lin-45(gf); dpy-20(e1282)IV*; SD806 *gaIS36[Hs::mpk-1(wt), Hs::mek]; him5(e1490)V*; MT8677 *ksr-1(n2526)X*; PS3352 *syIs50 (cdh-3::GFP)X; dpy-20(e1282)IV*.

Microscopy

Animals were examined with an Olympus BX51 epifluorescence microscope equipped with DIC optics, F-View camera (Soft Imaging System, 10×), Olympus PlanApo 60×/1.40 Oil Ph3 ∞/0.17 objective, Olympus U-RFL-T Hg burner, and filters ex HQ470/40, DM Q495LP, em HQ515/30. Images were processed using analySIS PRO 3.2 software (Soft Imaging System). Scoring the number of divided versus non-divided Pn.px and Pn.pxx cells was performed at the L3 stage.

RNA interference (RNAi) and transgene construction

For RNAi via ingested double-stranded RNAs, an *Xho*I-digested fragment of the full-length cDNA corresponding to F25H2.5 (*yk1105e04*) was cloned into pPD129.36 (a gift from A. Fire), and the construct obtained was transformed into HT115 (DE3) bacteria. RNAi experiments were performed at 25°C. To generate a translational fusion F25H2.5::GFP reporter, the following primers (5′-3′) were used: Promoter plus ORF, TTGGGGCGCGCCATCGGCGATCGCCTTCGCTCTCCATCGGCTTCG and TTTTGGGCCCATTATTAATTAACTCAGGCCGGCCATCAGCGGCCTTCGTAGACCCATGAGTTGATGAATGG; 3′UTR, TTGGGGCGCGCCATCGGCGATCGCATCTGCGGCCGCATCTGGCCGGCCTGAGTTAATTAATAAACTGATTGCTTATGTCTCCCG and TTTTGGGCCCGAACGATTTTCCAAGGTTCCAAC. The amplified fragments were digested with *Asc*I/*Not*I and *Fse*I/*Apa*I, respectively, and cloned into pRH21 (Hofmann et al., 2002). Subsequently, transgenic worms (strain TTV2) were generated by biolistic transformation using the *unc-119(ed3)* mutant genetic background and the *unc-119(+)* gene as a cotransformation marker. A single-copy integrated version was generated by cloning the insert into the MosSCI vector PCFJ151 (Addgene) (*Afl*II/*Spe*I sites) and injection-based transformation.

Western blot

Activated MAPK displays both a germline-specific band and a somatic band (Ohmachi et al., 2002). About 350 late L4 staged worms were picked and subjected to lysis. Probing for ERK and diphosphorylated ERK was performed using rabbit anti-ERK (K-23, Santa Cruz) and mouse anti-ERK (MAPK-YT, Sigma) antibodies at 1:2000 dilution. Mouse anti-tubulin antibodies (DM1A, Sigma; 1:4000) were used as loading controls. HRP-conjugated anti-rabbit (Jackson Immunochemicals; 1:10,000) and anti-mouse (DakoCytomation; 1:2000) were used as secondary antibodies.

MBP pulldown

ndk-1 and *ksr-2* inserts were generated from cDNAs by PCR using the following primers (5′-3′): *ndk-1*, CAGAAGATCTATGAGCAACACTGAGAGAACC and ATAGTTTAGCGGCCGCTTTCGTAGACCCATGAGTTG; *ksr-2*, CTGAGGATCCATGAGCGATGAAAAGAAGAAAAAGC and ATAGTTTAGCGGCCGCTAAACAGTGGATTCTCGTGTGC; murine *Ksr1*, CAGAGATCTATGGATAGAGCGGCGTTGCG and ATAGTTTAGCGGCCGCTCATCTTTGGATTACCGGACTCC. *ndk-1* was ligated into a modified pET vector (Novagen) and the GST::NDK-1::His6 protein was expressed in *E. coli* strain Rosetta pLysS. *ksr-2* was ligated into a modified pFastBac vector (Invitrogen). MBP::KSR-2::His6 and murine MBP::KSR1 proteins were expressed in the Sf9 cell line using the BAC-to-BAC baculovirus expression system. NDK-1 was purified using Ni affinity and GST chromatography techniques. The MBP pulldown assay was performed in 200 μl total volume of 20 mM Tris buffer (pH 8) containing 1 mM EDTA, 0.1% IGEPAL, 5 mM β-mercaptoethanol, 2 mM benzamidine, 0.25 mM PMSF, 0.15 mM NaCl. Each binding reaction contained 5 μM NDK-1 and 30 μl MBP resin (New England Biolabs) saturated with MBP::KSR::His_6. The reaction mixture was incubated at room temperature for 20 minutes, washed three times, then protein samples were analyzed by western blot using an anti-GST antibody (Cell Signaling). Control binding reaction contained MBP resin saturated with MBP protein only.

RESULTS

ndk-1, the sole *Caenorhabditis elegans* ortholog of group I NDPKs, is an essential gene

The *C. elegans* genome contains three open reading frames (ORFs), *F25H2.5*, *F55A3.6* and *Y48G8AL.15*, which show high sequence similarity to NDPKs (Bilitou et al., 2009). *F25H2.5* is the most closely related to group I NDPKs. The other two nematode NDPK paralogs, *F55A3.6* and *Y48G8AL.15*, are more divergent and belong to group II NDPKs. Here, we focused on F25H2.5, which shows 65% sequence identity and 85% overall similarity to NM23-H1 and NM23-H2 (Fig. 1A). NM23-H1 amino acids His118 and Ser120, which are reported to be essential for kinase activity (Steeg et al.,

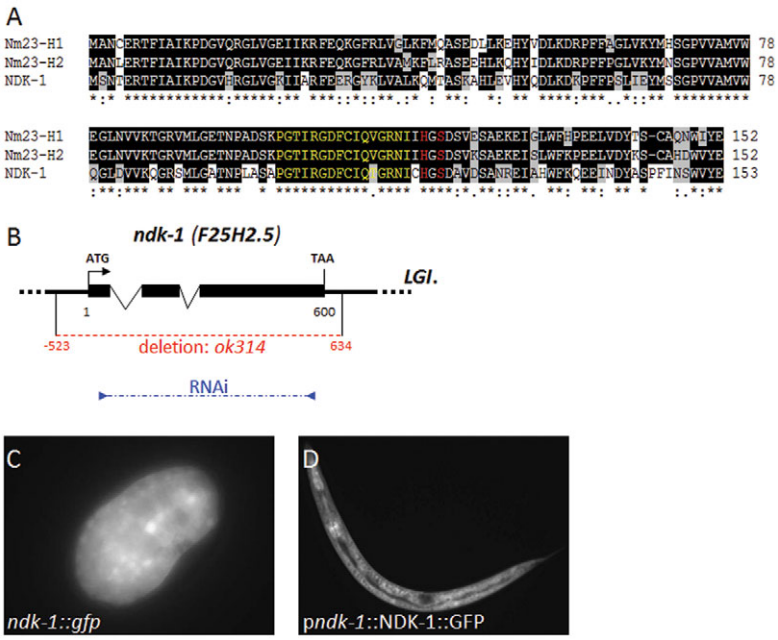

Fig. 1. *C. elegans ndk-1* is an essential gene. (**A**) Sequence alignment of human NM23-H1 (NME1), NM23-H2 (NME2) and *C. elegans* NDK-1 (F25H2.5) proteins. Identical and similar residues are highlighted with black and gray shading, respectively. NDK-1 shows 85% overall similarity to both NM23-H1 and -H2 isoforms. Amino acids His118 and Ser120 (red), which are essential for kinase activity and NDPK multimer formation, respectively, are conserved in these proteins. A 16 amino acid stretch N-terminal to the catalytic site at His118 (yellow) is also highly conserved. (**B**) Genomic structure of the *ndk-1* gene. Sequencing of the *ndk-1* full-length cDNA clone *yk1105* confirmed the exon-intron structure predicted by WormBase. The dotted red line shows the position of the *ok314* deletion, which includes the complete ORF of *ndk-1*, a 523 bp 5′ regulatory region and 34 bp of the 3′UTR. The position of primers used for generating the *ndk-1* RNAi clone is indicated in blue. (**C**) Ubiquitous expression of a transcriptional *ndk-1::gfp* reporter in a comma stage *C. elegans* embryo. (**D**) Expression of a functional translational fusion NDK-1::GFP reporter in an L2 stage larva.

2003) and NDPK multimer formation (Mocan et al., 2007), respectively, are conserved in the worm protein. A 16 amino acid stretch N-terminal to the catalytic site at His118 is also highly conserved (indicated by yellow lettering in Fig. 1A). Based on this sequence conservation, we named the *F25H2.5* gene *ndk-1* (*C. elegans* ortholog of *nucleoside diphosphate kinase-1*). Sequence analysis of the *ndk-1* full-length cDNA clone *yk1105* confirmed the exon-intron structure predicted by WormBase (Fig. 1B).

To assess the function of *ndk-1* in development, we analyzed the *ok314* 1157 bp deletion allele of *ndk-1*, which removes the entire *ndk-1* ORF, as well as 523 bp of upstream and 34 bp of downstream sequences (Fig. 1B). We backcrossed the *ok314* null allele five times to eliminate unlinked mutations and balanced it with *hT2qIs48* in order to allow for stable propagation of the *ndk-1(ok314)* mutation. Analysis of the progeny of *ok314/+* heterozygotes revealed that nearly 12% of *ok314* homozygotes die as embryos, while the remainder develop into sterile adults that display a protruding vulva phenotype (Pvl) (Table 1). In addition, we observed low penetrance Clear (Clr) and Constipation (Con) phenotypes in mutant adults (see below). The Clr phenotype was often coupled with a fluid-filled-like appearance to the affected worms. To confirm that this pleiotropic mutant phenotype associated with *ok314* is indeed caused by this deletion, we depleted NDK-1 by RNAi. Many RNAi-treated worms were sterile and had a Pvl phenotype, and the remainder produced a reduced number of progeny (Table 1). An integrated single-copy, *gfp*-labeled *ndk-1(+)* transgene (p*ndk-1*::NDK-1::GFP; see Materials and methods) was able to rescue the mutant *ndk-1(–)* phenotypes (Table 1). This rescue, together with the convergence of deletion and RNAi phenotypes, indicates that NDK-1 is required to form a properly developed vulva and for normal germline development. The weaker RNAi phenocopy is likely to be due to only partial depletion of NDK-1.

NDK-1 expression established by the aforementioned GFP fusion as well as by a transcriptional reporter construct converged, and expression was observed in different developmental stages, from embryonic through all larval stages to adulthood (Fig. 1C,D). During larval development, GFP expression was detected in the hypodermis, the intestine and body wall muscles, as well as in neurons residing in the ventral nerve cord, the head and the tail (Fig. 1D). The *ndk-1::gfp* reporter was ubiquitously expressed in the developing vulva tissue from mid-L3 larval stage until adulthood (Fig. 2, Fig. 3D).

ndk-1(–) mutants display defects in vulval development

We first analyzed the Pvl phenotype associated with *ndk-1(ok314)* mutants. The Pvl phenotype is characterized by the eversion of the vulval tissue and the formation of a single protrusion, and can be the consequence of misspecification of vulval cell fates, impaired vulval morphogenesis (Eisenmann and Kim, 2000) or partial cell cycle defects (O'Connell et al., 1998). The gross vulval morphology of homozygous *ndk-1(ok314)* mutants showed an aberration of the characteristic 'christmas tree' structure at the L4 larval stage; the vulval structure at this stage was not symmetrical, which was likely to be due to misspecification of certain vulval cell types (Fig. 3A,C), as indicated by the misexpression of vulval cell fate markers (see below).

Table 1. The penetrance of lethality, sterility and Pvl phenotype of *ndk-1* mutant worms

Genotype	Embryonic arrest (%)	Sterility of viable adults (%)	Pvl of viable adults (%)	*n*
wild type	<0.1	0	0	>1500
ndk-1(ok314)	12.3	100	100	1054
ndk-1(RNAi)	14.7*	88.2	79.1	980
ndk-1(ok314);ndk-1(+) (p*ndk-1*::NDK-1::GFP)	2.2	5.2	0	344

p*ndk-1*::NDK-1::GFP denotes a single-copy integrated *gfp*-labeled transgene that effectively rescues *ndk-1(–)* phenotypes. Pvl, protruding vulva phenotype. *n*, number of animals examined.
*The control (empty) RNAi vector causes ~5% embryonic lethality.

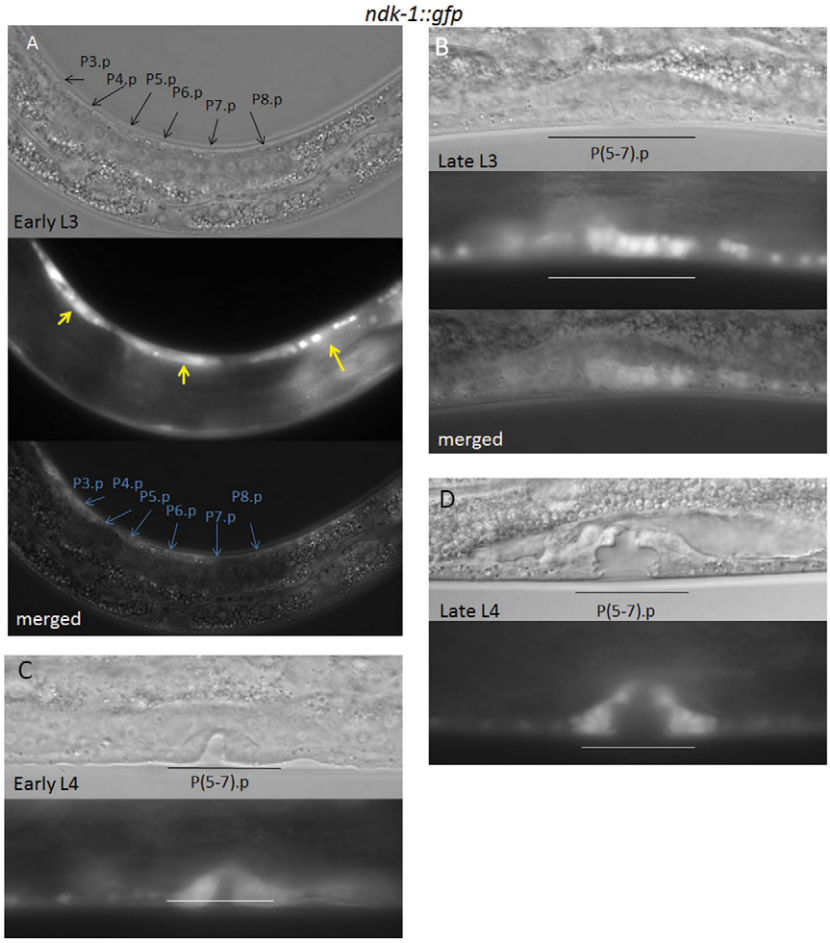

Fig. 2. *ndk-1* is expressed in the developing vulval tissue. (**A**) Expression of the *ndk-1::gfp* reporter in an early L3 larva. The position of vulval precursor cells (VPCs) is indicated by black and light blue arrows on the DIC and merged images, respectively. At this developmental stage, NDK-1 reporter expression is not detected in VPCs. Instead, hypodermal seam cells show reporter expression (yellow arrows). Note that many cells from the ventral nerve cord are also fluorescent, possibly obscuring a lower level of expression in VPCs. (**B**) In late L3, NDK-1 accumulates in the VPC descendants. P(5-7).pxx cells are underlined. (A,B) Top, DIC image; middle, the corresponding fluorescence image; bottom, merge. (**C**) *ndk-1* expression in the developing vulval tissue at the early L4 larval stage. (**D**) The expression of *ndk-1* in the vulval cells of a late L4 stage larva. (C,D) Top, DIC image; bottom, the corresponding fluorescence image.

During *C. elegans* vulval development, the induced VPCs P(5-7).p undergo three rounds of cell division in response to the inductive signal and generate distinct cell types: vulA, vulB1, vulB2, vulC and vulD cells are descendants of P5.p and P7.p and are referred to as secondary lineages, whereas vulE and vulF cells are great-granddaughters of P6.p and referred to as primary cells (Fig. 3A). At the mid-L4 larval stage, the developing vulva consists of 22 cells, which subsequently migrate and undergo cell fusion events to eventually form the adult vulval structure. To analyze the nature of the Pvl phenotype of *ndk-1(ok314)* mutant hermaphrodites, we monitored vulval cell types using specific markers for individual vulval cell fates (Fig. 3E-H) (Inoue et al., 2002). *cdh-3* (cadherin family) encodes a cadherin-related protein, and *cdh-3::gfp* can serve as a marker for vulC, vulD, vulE and vulF cells (Fig. 3E,F). We found that among the cells conferring secondary fates, *cdh-3::gfp* expression in both vulD and vulC cell types was, with variable penetrance, missing in the mutant vulva. The lack of *cdh-3::gfp* expression in vulD was detected in 9% of *ndk-1(–)* mutants, whereas missing vulC cells were observed in 36% of cases (n=98). *cdh-3::gfp* expression was also missing in vulE cells in 36% of the mutants, and in vulF cells in 18%, showing that *ndk-1(ok314)* animals also lack cells belonging to primary lineages (Fig. 3G,H). *egl-17* (egg-laying defective) encodes an fibroblast growth factor (FGF) ligand and is expressed specifically in vulC and vulD at the mid-L4 larval stage (Fig. 3I). In 96% of the *ndk-1(ok314)* hermaphrodites (n=145), vulC and/or vulD cells failed to express the *egl-17::gfp* reporter (Fig. 3J).

We also considered that the failure of cell type-specific gene expression, especially during late stage vulva morphogenesis, might be an indirect consequence of a reduced number of cell cycles occurring during vulva development. We thus counted the number of vulva cells in *ndk-1(ok314)* mutants, and found an average of 20±1 cells (n=98) compared with the 22 cells observed in the wild type. We thus conclude that reduced cell cycle progression might also contribute to the reduced cell type-specific gene expression, but is unlikely to solely account for this defect.

EGL-17/FGF is a downstream target of EGFR/Ras/MAPK signaling during vulval development (Cui and Han, 2003). Its accumulation in the P6.p descendants (daughters/granddaughters), in which signaling normally occurs, can therefore serve as a marker for Ras-dependent vulval fate induction (Burdine et al., 1998). This prompted us to monitor EGL-17::GFP accumulation in the P6p.xx granddaughters at the late L3 stage. We found markedly reduced levels or even the absence of EGL-17 in these cells in the *ndk-1(–)* mutant background, as compared with the wild-type genetic background (Fig. 4A-C). From these data, we conclude that NDK-1 may be necessary for the proper adoption of vulval cell fates, consistent with the strong NDK-1 expression observed starting from the late L3 stage (Fig. 2).

NDK-1 functions downstream of, or in parallel to, LIN-45 and upstream of MEK-2 and MPK-1 to affect vulval development

The observation that transcriptional induction of a known Ras/MAPK target, EGL-17/FGF, is alleviated in *ndk-1(–)* mutants,

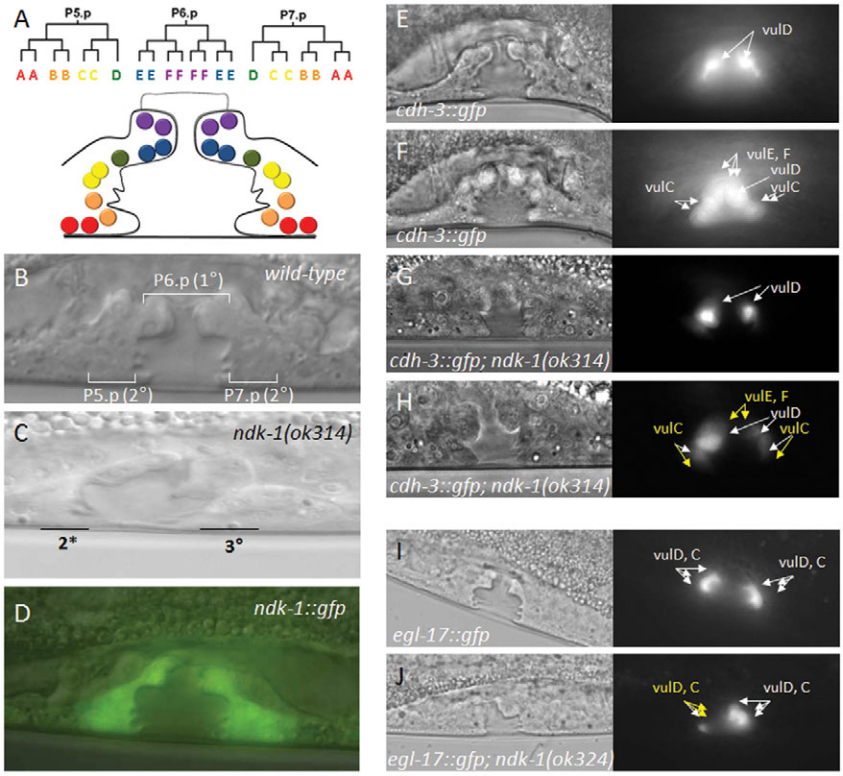

Fig. 3. *ndk-1(ok314)* mutants display defects in vulval development. (**A**) The wild-type, mid-L4 stage vulva is composed of 22 cells, which can be grouped into seven cell types (vulA, B1, B2, C, D, E and F). These cells are the great-granddaughters of P5.p-P7.p VPCs (blue and violet circles, primary lineages; red, orange, yellow and green circles, secondary lineages). (**B**,**C**) The vulva structure of a wild-type (N2) mid-L4 stage larva (B) and an *ndk-1(ok314)* mutant mid-L4 stage larva (C). The mutant vulval structure is not symmetrical. (**D**) A transcriptional *ndk-1::gfp* reporter is expressed in the developing vulva of an L4 stage larva. (**E-H**) *cdh-3::gfp* is a marker for vulD, C, E and F cells (white arrows) at the L4 stage. Each figure consists of a fluorescent image (right) of *cdh-3::gfp* expression and a DIC image (left) of the corresponding focal plane. (E,F) *cdh-3::gfp* expression in a wild-type worm in two different focal planes: the focal plane of vulD cells (E) and that of vulC, E and F cells (F). (G,H) In an *ndk-1(ok314)* homozygote, vulD cells are present (G, white arrows), but vulE and F cells are missing (H, yellow arrows). (**I**,**J**) Expression pattern of the Ras/MAPK pathway target gene *egl-17* in a wild-type mid-stage L4 larva (I) and in an *ok314* mutant L4 stage larva (J). Both comprise a fluorescent image (right) of *egl-17::gfp* expression and a DIC image (left) of the corresponding focal plane. The *ndk-1* mutant shows reduced expression of *egl-17::gfp*, indicating that Ras/MAPK signaling is inhibited in the *ndk-1(–)* mutant background; white arrows indicate correctly specified vulval cells, yellow arrows show the position of non-fluorescent vulval cells that would normally express *egl-17*.

prompted us to examine whether *ndk-1* might generally affect Ras/MAPK signaling. The *C. elegans* vulva induction pathway provides a unique experimental system, as differences in the level of MAPK signaling can be measured by scoring for the formation of a reduced or enhanced number of vulval structures.

The single vulva-like structure in *ndk-1(ok314)* worms indicates that a basal level of Ras/MAPK signaling needed for vulva induction still occurs in these mutants. We thus analyzed double-mutant combinations to see whether, in these genetically sensitized backgrounds, the extent of Ras/MAPK signaling is modified *in vivo*. We performed a genetic epistasis analysis and examined the phenotypes of *ndk-1(ok314)* mutants combined with various mutants defective in different steps of the Ras/MAPK signaling pathway. First, the *let-23(n1045)* hypomorphic mutant, which affects an EGF receptor, was crossed with *ndk-1(ok314)*. At 15°C, *let-23(n1045)* single-mutant hermaphrodites are Vul (with 96% penetrance), whereas *ndk-1(ok314)* single-mutant adults exhibit a Pvl phenotype. We found that *ndk-1(ok314);let-23(n1045)* double-mutant adults have a fully penetrant Vul phenotype that affects 100% of the adults analyzed (the average number of induced VPCs in the double mutants was 0.09; n=11), consistent with the hypothesis that Ras/MAPK signaling might be further attenuated in the *ndk-1(–)* background. In addition, 43% of *ndk-1(–);let-23(–)* double mutants (n=35) were unable to develop into adults as they arrested development at earlier (L1-L3) larval stages. By contrast, larval lethality was not observed in either single mutant. This genetic interaction suggests that the *ndk-1(ok314)* mutation enhances the severity of the Let-23(n1045) phenotype (Vul adults) towards a Let-23 null phenotype [rod-like L1 arrest (Yochem et al., 1997)], and represents additional evidence for reduced signaling efficiency in *ndk-1(–)* mutants.

To further verify this notion and to start establishing epistatic relationships, we next crossed *ndk-1(–)* mutants with animals in which Ras/MAPK signaling is hyperactivated. The *ndk-1* mutation *ok314* significantly reduced the number of excessive vulval protrusions (the Muv multivulva phenotype) in *let-23/EGFR* and *let-60/RAS* gain-of-function mutants (Table 2). These data suggest that *ndk-1* acts downstream of *let-23* and *let-60* to enhance Ras/MAPK signaling. To more precisely place the function of NDK-1 in the Ras/MAPK signaling pathway, we also tested its epistatic relationship with *lin-45/Raf*. *lin-45* overexpression

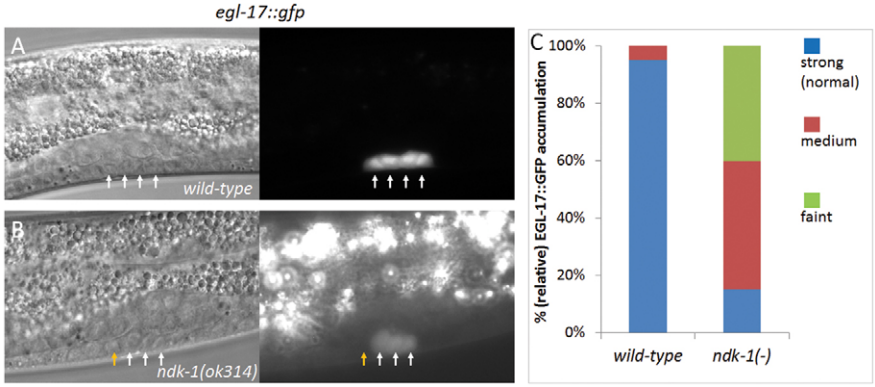

Fig. 4. *EGL-17::GFP* expression is much reduced in P6p.xx cells of *ndk-1(–)* mutants. The accumulation of EGL-17/FGF, a marker for Ras-dependent vulval fate induction (*egl-17* is an EGFR/Ras/MAPK signaling target), in the P6.p granddaughters, in which signaling actually occurs. (**A**) EGL-17::GFP expression in a wild-type L3 larva. The four P6.p descendants (P6p.xx, arrows) strongly accumulate EGL-17. (**B**) EGL-17::GFP expression in a *ndk-1(–)* mutant L3 larva. The expression intensity is much reduced compared with the wild type (the image was taken with a much longer exposure time than that used for the control, as indicated by the much brighter background of gut autofluorescence). In addition, one of the P6.p granddaughters (the yellow arrow) fails to accumulate EGL-17 in this specimen. (A,B) DIC images are on the left, the corresponding fluorescent images on the right. (**C**) Quantification of expression intensity of EGL-17::GFP in P6p.xx cells. *n*=20; for comparing levels of faint expression between wild type and *ndk-1(–)*: *P*<0.001, unpaired Student's *t*-test.

conferred by the transgene *kuIs57* leads to a Muv phenotype (Yoder et al., 2004). We found that this phenotype is significantly reduced by the *ndk-1(–)* mutation, showing that NDK-1 functions downstream of LIN-45 in the vulva induction pathway (Table 2). By contrast, the excessive vulva induction conferred by overexpression of downstream components of the pathway, such as *mek-2/MEK* and *mpk-1/MAPK*, could not be suppressed by the *ndk-1(ok314)* deletion (Table 2). Thus, NDK-1 is likely to function upstream of MEK-2 and MPK-1. Consistently, the ectopic vulva formation conferred by deleting *lin-1* and *lin-31*, which encode MPK-1 targets, was not suppressed by the *ndk-1* deletion (Table 2). The results of this epistasis analysis were further confirmed by scoring the average number of induced VPCs in the single Muv mutants and the corresponding double mutants (Table 2). In summary, these experiments suggest that NDK-1 is required for the full activation of Ras/MPK-1 signaling but not for Ras/MPK-1 signaling per se.

The epistasis analysis described above, together with the reduced expression of the LIN-1/LIN-31 target *egl-17*/*FGF* (Cui and Han, 2003), indicates that the extent of Ras/MAPK signaling might be dampened in *ndk-1(ok314)* mutants (Fig. 3I,J, Fig. 4). To confirm this, we directly measured the level of activated, threonine and tyrosine phosphorylated MAPK in *C. elegans* extracts using phospho-specific MAPK antibodies. *C. elegans* MPK-1/MAPK is expressed in two isoforms: a larger isoform that is expressed in the germline and a smaller isoform that is restricted to somatic tissues (Fig. 5) (Ohmachi et al., 2002). We found expression of the germline isoform to be missing in the *ndk-1(ok314)* mutant, consistent with the largely stunted germline development observed in *ndk-1(ok314)* homozygotes. The dramatic reduction of activated MAPK in the soma demonstrates that MAPK signaling, but not the basal protein level, is reduced in all somatic tissues of animals defective for NDK-1 (Fig. 5, middle panel).

Table 2. Epistasis analysis performed between vulval determination genes and *ndk-1*

Genotype	Average number of VPCs induced	*n*	Muv (%)	*n*	*P*-value
wild type	3.0	>200	0	>200	
ndk-1(ok314)	2.9	52	0	100	
let-23(sa62)	4.8	17	96	54	
let-23(sa62);ndk-1(ok314)	3.6	15	61.9	42	<0.0001
let-60(n1700)	4.3	20	92	103	
let-60(n1700);ndk-1(ok314)	3.3	42	23	65	<0.0001
*lin-45(gf)**	4.3	15	94	33	
*lin-45(gf);ndk-1(ok314)**	3.6	17	42	33	<0.0001
hs::mpk-1;hs::mek‡	3.5	18	32.4	74	
hs::mpk-1;hs::mek;ndk-1(ok314)‡	3.5	37	36	36	0.6985
lin-1(e1275)	5.8	22	93	40	
lin-1(e1275);ndk-1(ok314)	5.8	20	88	45	0.8231
lin-31(n1053)	5.1	18	77.5	49	
lin-31(n1053);ndk-1(ok314)	5.0	16	79.5	44	0.3741

Epistasis analysis suggests that *ndk-1* acts downstream of *lin-45*/*Raf* and upstream of *mpk-1*/*MAPK* in the Ras/MAPK cascade. Epistasis analysis was carried out by scoring the average number of induced VPCs at the L3 larval stage and by counting the percentage of adult worms with a multivulva (Muv) phenotype as examined under a dissecting microscope. The distribution of Muv and non-Muv adults was examined using a chi-squared test. *P*-values derived from comparing data of single Muv mutants and the corresponding double mutants were calculated using VassarStats (http://vassarstats.net/tab2x2.html). *n*, number of animals examined.
*The transgene *kuIs57* was applied. *gf* denotes a *lin-45* transgene, *kuIs57*.
‡The strain *gaIs36* was used; *hs* denotes a heat shock promoter.

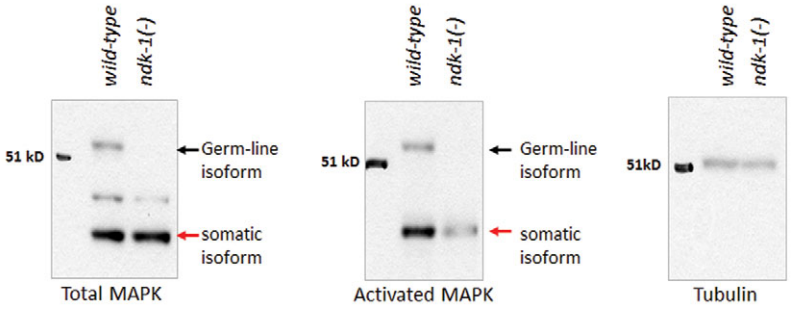

Fig. 5. Ras/MAPK signaling is inhibited in the *ndk-1(–)* mutant background. Analysis of total and diphosphorylated MAPK levels of wild-type and *ndk-1(ok314)* worms by western blotting. Black arrows indicate the germline-specific (55 kDa) isoform of MAPK; red arrows show the somatic (45 kDa) isoform of MAPK. As a control for loading, the blot was reprobed using anti-tubulin antibody. The mutant germline completely lacks MAPK. The level of total MAPK in the soma is comparable in mutant and wild-type worms. However, the level of activated MAPK is severely reduced in *ndk-1(ok314)* mutants.

The Ksr-1 and Ksr-2 phenotypes are exacerbated in the *ndk-1(ok314)* background

Human NM23-H1 was found to interact with KSR1 *in vitro*, suggesting that NM23-H1 affects Ras/MAPK signaling through modulating KSR activity (Hartsough et al., 2002; Salerno et al., 2005). KSR1 is a conserved scaffold protein that is required for signaling through the Ras/MEK signaling module, but the function of the NM23-KSR1 interaction has not been determined *in vivo*. In addition, unlike data obtained from human cell cultures, genetic results presented here demonstrate a stimulatory effect of NDK-1 on Ras/MAPK signaling in somatic tissues, and we wondered whether NDK-1 might act by modulating the activity of KSR proteins. The *C. elegans* genome encodes two KSR paralogs, KSR-1 and KSR-2, which function redundantly in most Ras-related processes (Kornfeld et al., 1995; Sundaram and Han, 1995; Ohmachi et al., 2002; Sundaram et al., 1996). KSR-1 and KSR-2 share 26% and 31% sequence identity with murine KSR1 (Ohmachi et al., 2002). Our genetic results indicated that *ndk-1* occupies a similar epistasis position in the Ras/MAPK signaling pathway as that reported for KSRs, which function downstream of *lin-45* and upstream of *mek-2* and *mpk-1* to affect vulval development (Table 2) (Yoder et al., 2004). Therefore, we assessed genetic interactions between *ndk-1* and the two worm KSR paralogs.

ndk-1(ok314);ksr-1(n2526) double-mutant animals developed into sterile adults showing a Pvl phenotype, as it is the case for the *ndk-1(ok314)* single mutant. However, the 33% penetrant egg-laying defective (Egl) phenotype associated with the *ksr-1* mutation was enhanced to 77% in the *ndk-1(ok314)/+* heterozygous *ksr-1(n2526)* strain (n=125; Table 3). The Egl phenotype of *ksr-1(n2526)* single mutants is due to a defect in sex myoblast migration, a process that also relies on Ras/MAPK signaling (Sundaram et al., 1996). By contrast, vulval development in *ksr-1(n2526)* single mutants appears normal. The enhanced Egl phenotype observed in *ndk-1(ok314)/+;ksr-1(n2526)* worms might therefore arise either from abnormal sex myoblast migration or from defects associated with the morphogenesis of the vulva. To address this issue, we checked vulval morphology in the F1 progeny of *ndk-1(ok314)/+;ksr-1(n2526)* hermaphrodites. Abnormal vulval structures were observed in 60% of L3-L4 stage worms (n=20; data not shown). Thus, given that only 25% of these animals are expected to be homozygous for the *ndk-1(ok314)* mutation, the high penetrance of abnormal vulval structures suggests that the vulva development of *ndk-1(ok314)/+;ksr-1(n2526)* worms is abnormal [note that *ksr-1(n2526)* mutants form a wild-type-like ‘christmas tree’ in L4]. To gain a deeper insight into the vulva development of *ndk-1(ok314)/+;ksr-1(n2526)* worms, we counted the number of induced VPCs in these animals (the average number of induced VPCs was 2.83; n=12) and found that they possess a mild induction defect similar to *ndk-1(–)* single mutants. Thus, the enhanced egg-laying defect might be due to a combination of a defective vulva and abnormal sex myoblast migration. Irrespectively, we convincingly show a genetic interaction between *ndk-1* and *ksr-1*.

We next focused on possible genetic interactions between *ndk-1* and *ksr-2*. Given that both genes are located on chromosome I, we generated a *cis*-heterozygous *ndk-1(ok314) ksr-2(dx27)/++* strain balanced with *hT2qIs48*, which carries *gfp* as a marker [*ndk-1(ok314)ksr-2(dx27)/hT2qIs48*]. This strain segregates GFP-positive larvae and adults only, indicating that (non-GFP) *ndk-1 ksr-2* homozygous double-mutant worms are embryonic lethal (Table 3).

To further assess genetic interactions between *ksr-2* and *ndk-1*, we analyzed *ndk-1(ok314) ksr-2(dx27)/+ ksr-2(dx27)* worms, expecting that Ndk-1 phenotypes might be enhanced. In addition to sterility and the Pvl phenotype already observed in the *ndk-1(ok314)* single mutant, these animals also showed 100% penetrant clear (Clr) and constipation (Con) phenotypes (Fig. 6A, Table 3). Clr and Con

Table 3. *ndk-1* shows a genetic interaction with both *ksr-1* and *ksr-2*

Genotype	*n*	Viability (%)	Adults (%)				
			Ste	Pvl	Clr	Con	Egl
ndk-1(ok314)	200	88	100	100	11	14	0
ksr-1(n2526)	130	100	0	0	0	0	33
ndk-1(ok314)/+;ksr-1(n2526)	125	ND	0	0	0	0	77
ndk-1(ok314);ksr-1(n2526)	55	100	100	80	9	ND	0
ndk-1(RNAi);ksr-1(n2526)	116	ND	71	74	8.6	0	0
ksr-2(dx27)	70	100	100	9	0	0	0
ndk-1(ok314/+) ksr-2(dx27)	40	ND	100	40	100	100	0
ndk-1(ok314) ksr-2(dx27)	–	0	–	–	–	–	–

The Ndk-1 phenotype is exacerbated in the *ksr-2(–)* background. *ksr-2(dx27) ndk-1(ok314)* homozygotes are not viable. Clear (Clr) and constipation (Con) phenotypes of *ndk-1(ok314)* homozygotes are enhanced in the presence of a *ksr-2(dx27)* allele. Pvl, protruding vulva; Ste, sterility; Egl, egg-laying defective. *n*, number of animals examined. ND, not determined.

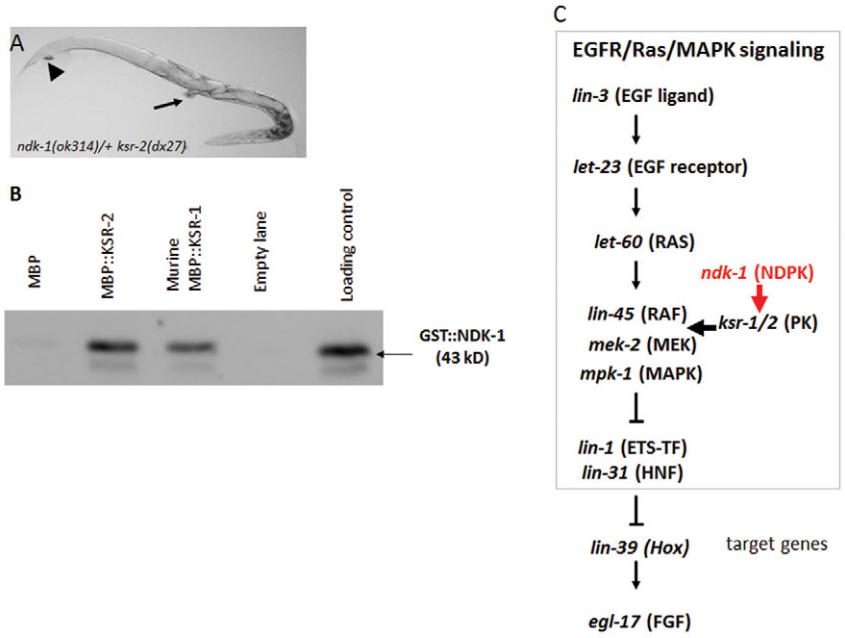

Fig. 6. NDK-1 interacts with KSRs. (**A**) *ndk-1(ok314) ksr-2(dx27)/+ ksr-2(dx27)* animals are clear, have a protruding vulva (arrow) and display a constipation (arrowhead) phenotype. (**B**) *In vitro* pulldown assay shows that NDK-1 binds to KSR-2 and to murine KSR1. Western blot was performed with anti-GST antibody. Lane 1, resin-bound MBP and GST::NDK-1 as a negative control; lane 2, MBP::KSR-2 and GST::NDK-1; lane 3, MBP::KSR1 (mouse protein) and GST::NDK-1; lane 5, GST::NDK-1 as positive control for loading. (**C**) Epistatic position of *ndk-1* in Ras/MAPK signaling. *ndk-1* acts downstream of *lin-45/Raf* and upstream of *mpk-1/MAPK* in the Ras/MAPK pathway during vulval development. We propose that NDK-1 activates the Ras/MAPK cascade through modification of the activity of KSR scaffolds.

phenotypes were also observed in *ndk-1(ok314)* single mutants, although with a low penetrance (Table 3). The Clr phenotype can be associated with defects in protein degradation in muscles (Szewczyk and Jacobson, 2003) and is reported to result from excessive FGFR/Ras/MAPK signaling (Kokel et al., 1998). However, decreased EGFR/Ras/MAPK activity in the excretory duct can also result in arrested Clr animals (Yochem et al., 1997; Abdus-Saboor et al., 2011). The Con phenotype is also linked to excessive Ras/MAPK signaling as implicated in the defense mechanism against pathogens (Nicholas and Hodgkin, 2004). However, a reduced level of Ras/MAPK signaling can also lead to a Con phenotype (Nicholas and Hodgkin, 2004). Nevertheless, these genetic interactions indicate that NDK-1 might modulate KSR activity, which in turn affects Ras/MAPK signaling.

To assess whether modulation of KSR activity by NDK-1 might be mediated by a direct interaction, we tried to establish whether KSR and NDK-1 proteins can directly interact. Given that we are working in an *in vivo* system in which key biochemical interactions are predicted to occur in only a subset of cells, we focused on *in vitro* interactions using pulldown experiments with recombinant GST::NDK-1 and MBP::KSR fusion proteins. We managed to express *C. elegans* KSR-2, but could not express worm KSR-1 and therefore used mouse KSR1. These pulldown experiments demonstrate that both murine KSR1 and worm KSR-2 interact with NDK-1 (Fig. 6B). Thus, the increased level of Ras/MAPK signaling conferred by NDK-1 might reflect direct modulation of KSR activity by NDK-1.

DISCUSSION

In this study we characterized *ndk-1*, the *C. elegans* ortholog of human *NM23-H1/H2* (*NME1/2*). *ndk-1* knockouts display sterility and a protruding vulva. By analyzing the vulva phenotype, we demonstrated that both primary and secondary vulval cell fates are affected in *ndk-1(–)* mutant hermaphrodites, raising the hypothesis that *ndk-1* influences the execution and/or stage-specific gene expression of several vulval cell types. In addition, we assessed whether *ndk-1* modifies Ras/MAPK signaling. We initially focused on the inductive (Ras) signaling pathway, which is needed to initiate vulva development at the early L3 stage (Sternberg, 2005). Epistasis analysis performed with *ndk-1* and Ras pathway mutants demonstrated that *ndk-1* acts downstream of, or in parallel to, *lin-45/Raf*, and upstream of *mek-2/MEK* and *mpk-1/MAPK* to affect the formation of the vulva tissue. NDK-1 deficiency suppressed the extent of multiple vulva formation conferred by *let-23(gf)*, *let-60(gf)* and *lin-45(gf)* gain-of-function (*gf*) mutants (Table 2). Conversely, the *ndk-1(ok314)* mutation, although not itself causing a reduction in the number of vulva structures formed, nevertheless results in a reduced level of MAPK signaling. The level of *egl-17*/*FGF*, a known MAPK target (Cui and Han, 2003), is reduced in *ndk-1* mutants in the developing vulval tissue (Fig. 3I,J, Fig. 4), similar to the global levels of activated MAPK (Fig. 5). In summary, NDK-1 is necessary for proper MAPK activation in somatic tissues.

We noted that our *ndk-1* reporter only showed strong expression from the late L3 stage onwards. We speculate that the effects of NDK-1 in the vulva induction pathway only require a very low level of expression that is not detectable by our reporter. The vulva induction system provides the unique possibility to uncover and characterize modulators of MAPK signaling; even so single mutants similar to *ndk-1*, such as *sur-6/PP2A* or *par-1*, display only mild (e.g. Pvl) or no vulval phenotype on their own (Sieburth et al., 1999; Hurd and Kemphues, 2003; Yoder et al., 2004).

As NDPKs have been associated with diverse biological processes in other model systems, it is not surprising that NDK-1 also has multiple functions in the worm. Besides modulating Ras/MAPK signaling, NDK-1 may also act in later processes during vulval development, such as cell fate execution, as strong NDK-1 expression can be detected from the late L3 stage onwards, stages at which fate patterning of the VPC daughter cells occurs. Defects in the secondary vulval lineages of *ndk-1(–)* mutants (Fig. 3) raised the question of whether NDK-1 plays a role in LIN-12/Notch-mediated lateral signaling, which is essential for secondary cell fate specification (Greenwald, 2005). However, depleting NDK-1 in animals with hyperactive *lin-12* function did not alter vulval induction, as compared with *lin-12(gf)* mutants (data not shown).

KSRs act as scaffold proteins in the Ras/MAPK cascade and assemble Raf/MEK complexes, thereby facilitating MAPK activation (Kolch, 2005). *C. elegans* KSR-1 and KSR-2 function redundantly in most Ras-related processes in somatic tissues, such

as the vulva tissue, the excretory system and the male spicules, whereas KSR-2 acts alone in the germline to ensure meiotic progression (Ohmachi et al., 2002). Since *ndk-1* and the KSR paralogs operate at the same level in the Ras/MAPK pathway, and they all contribute to the process of MAPK activation, we generated *ndk-1(–);ksr-1(–)* and *ndk-1(–)ksr-2(–)* double knockouts in order to test potential genetic interactions between *ndk-1* and the KSR genes. We conclude from these results that NDK-1 may act together with both KSRs during development, as depletion of either *ksr-1* or *ksr-2* in the *ndk-1(–)* background results in enhancement of the single-mutant phenotypes. In the progeny of *ndk-1(–)/+;ksr-1(–)* animals we saw enhancement of the single *ksr-1(–)* mutant phenotype (Egl). By contrast, in *ndk-1(–)/+ ksr-2(–)* worms, characteristics of *ndk-1*, such as the Clr and Con phenotypes, as well as embryonic lethality are exacerbated. Embryonic lethality of homozygous *ndk-1(–)* mutants (50%) becomes fully penetrant in the *ksr-2* mutant background.

ksr-1 and *ksr-2* were reported to act redundantly in the development of the male spicule and in the formation of the excretory duct (Ohmachi et al., 2002). We observed that *ndk-1(ok314)* males exhibit an abnormal tail without rays (100%, *n*=36), suggesting that NDK-1 also participates in male tail development. However, *ndk-1* mutants display no L1 larval lethality, a Ras phenotype reported to be linked to the loss of the excretory duct cell (Yochem et al., 1997). A possible explanation is that excretory duct cell specification might be mediated redundantly by the worm NDPK paralogs or that the maternal contribution of NDK-1 is sufficient for this developmental event to occur. Alternatively, MAPK signaling needed for excretory duct function might not require NDK-1. Analysis of *ndk-1(–)/+ ksr-2(–)* animals revealed the enhancement of Clr and Con phenotypes. At present we cannot explain why the *ndk-1* mutation enhances the Clr phenotype in a *ksr-2(–)* mutant background. The cause of the 10% penetrant Clr phenotype in *ndk-1(–)* single mutants and its enhancement by *ksr-2(–)* will need further investigation.

Human NM23-H1 was shown to bind to KSR1 in tissue culture models (Hartsough et al., 2002; Salerno et al., 2005; Tso et al., 2013), and *NM23-H1* overexpression in those cells resulted in reduced levels of MAPK signaling, the importance of which has not been demonstrated *in vivo*. Another study also suggested that increased levels of NM23-H2 blocks the ERK pathway (Lee et al., 2009). Here, we provide a compelling case that NDK-1 affects Ras/MAPK signaling at the level of KSRs.

In contrast to previous studies on mammalian cell lines, we found that NDK-1 promotes rather than suppresses Ras/MAPK signaling. Given that NDK-1 directly interacts with KSR-2, and possibly with KSR-1, we consider it likely that NDK-1 modifies the function of KSR scaffolds. We postulate that this modification alters KSR activity but is not absolutely essential for its function, as the *ndk-1(ok314)* mutation moderately decreases activated somatic MAPK levels and vulval induction in Ras hyperactive genetic backgrounds. It was previously reported that mouse KSR1 harbors 14-3-3 domain binding sites (Ser297 and Ser392, numbered according to the mouse KSR1 sequence) that are involved in KSR scaffold regulation in mammals (Müller et al., 2001). Comparison of mammalian and worm KSR sequences, however, reveals that Ser297 and Ser392 are not evolutionary conserved among different KSR proteins (Ohmachi et al., 2002). Overall, these findings suggest that KSR scaffold proteins could play diverse and context-dependent physiological roles in regulatory circuits controlling MAPK activation. Further studies are needed to dissect the molecular mechanism by which worm NDK-1 mediates the regulation of MAPK activity.

Earlier studies demonstrated that Nm23 proteins regulate neuronal differentiation in *Xenopus* and in cell lines (Mochizuki et al., 2009). Studies on knockout mice have shown that *Nm23-M1* (*Nme1*) mutant females cannot feed their pups due to growth retardation of the mammary glands and defects in the final step of mammary duct maturation of the nipple leading to duct obstruction (Deplagne et al., 2011). These genetic data are consistent with the prevailing idea that Nm23 proteins are involved in cell growth and differentiation. Our present data demonstrate that NDK-1/NM23-H1 controls differentiation through enhancing Ras/MAPK signaling. Activation of Ras/MAPK signaling by NDK-1/NDPK might be relevant in ovarian, prostate and pancreatic cancers in which Nm23 proteins are overexpressed (Harłozińska et al., 1996; Igawa et al., 1994; Andolfo et al., 2011; Takadate et al., 2012).

Acknowledgements
We thank M. V. Sundaram and Y. Kohara for cDNA clones; M. Han, A. Hajnal and the *Caenorhabditis* Genetics Center (which is funded by the National Institutes of Health) for nematode strains; T. Korcsmáros for preparing Fig. 2D; and Cs. Verasztó for statistical analysis.

Funding
This work was supported by the OTKA Hungarian Scientific Research Fund [PD75477 to K.T.-V.] T.V. is supported by OTKA [K109349]. A.M. is supported by the Wellcome Trust [069150]. A.G. is a Wellcome Trust Senior Research Fellow [0909444/Z/09/Z]. N.M. and E.P. were supported by Parkinson's UK [H-0709] and CRUK [C11852/A8052] PhD fellowships. K.T.-V., T.V. and A.R. are grantees of the János Bolyai Scholarship of the Hungarian Academy of Sciences. A.R. is a Wellcome Trust International Senior Research Fellow [081665/Z/06/Z]. The work was also supported by the 'Lendület' grant from the Hungarian Academy of Sciences to A.R. Deposited in PMC for immediate release.

Competing interests statement
The authors declare no competing financial interests.

Author contributions
K.T.-V., A.M., A.G. and T.V. designed research; N.M., L.F., E.P., A.A., T.V. and K.T.-V. performed research; A.R., A.G. and K.T.V. analyzed data; K.T.-V., A.M., A.G. and T.V. wrote the paper.

References

Abdus-Saboor, I., Mancuso, V. P., Murray, J. I., Palozola, K., Norris, C., Hall, D. H., Howell, K., Huang, K. and Sundaram, M. V. (2011). Notch and Ras promote sequential steps of excretory tube development in C. elegans. *Development* **138**, 3545-3555.

Andolfo, I., De Martino, D., Liguori, L., Petrosino, G., Troncone, G., Tata, N., Galasso, A., Roma, C., Chiancone, F., Zarrilli, S. et al. (2011). Correlation of NM23-H1 cytoplasmic expression with metastatic stage in human prostate cancer tissue. *Naunyn Schmiedebergs Arch. Pharmacol.* **384**, 489-498.

Biggs, J., Hersperger, E., Steeg, P. S., Liotta, L. A. and Shearn, A. (1990). A Drosophila gene that is homologous to a mammalian gene associated with tumor metastasis codes for a nucleoside diphosphate kinase. *Cell* **63**, 933-940.

Bilitou, A., Watson, J., Gartner, A. and Ohnuma, S. (2009). The NM23 family in development. *Mol. Cell. Biochem.* **329**, 17-33.

Burdine, R. D., Branda, C. S. and Stern, M. J. (1998). EGL-17(FGF) expression coordinates the attraction of the migrating sex myoblasts with vulval induction in C. elegans. *Development* **125**, 1083-1093.

Cui, M. and Han, M. (2003). Cis regulatory requirements for vulval cell-specific expression of the Caenorhabditis elegans fibroblast growth factor gene egl-17. *Dev. Biol.* **257**, 104-116.

Dammai, V., Adryan, B., Lavenburg, K. R. and Hsu, T. (2003). Drosophila awd, the homolog of human nm23, regulates FGF receptor levels and functions synergistically with shi/dynamin during tracheal development. *Genes Dev.* **17**, 2812-2824.

Deplagne, C., Peuchant, E., Moranvillier, I., Dubus, P. and Dabernat, S. (2011). The anti-metastatic nm23-1 gene is needed for the final step of mammary duct maturation of the mouse nipple. *PLoS ONE* **6**, e18645.

Desvignes, T., Pontarotti, P., Fauvel, C. and Bobe, J. (2009). Nme protein family evolutionary history, a vertebrate perspective. *BMC Evol. Biol.* **9**, 256.

Eisenmann, D. M. and Kim, S. K. (2000). Protruding vulva mutants identify novel loci and Wnt signaling factors that function during Caenorhabditis elegans vulva development. *Genetics* **156**, 1097-1116.

Greenwald, I. (2005). LIN-12/Notch signaling in C. elegans. In *WormBook: The Online Review of C. elegans Biology* (ed. The C. elegans Research Community). doi/10.1895/wormbook.1.6.1, http://www.wormbook.org.
Harłozińska, A., Bar, J. K. and Gerber, J. (1996). nm23 expression in tissue sections and tumor effusion cells of ovarian neoplasms. *Int. J. Cancer* **69**, 415-419.
Hartsough, M. T., Morrison, D. K., Salerno, M., Palmieri, D., Ouatas, T., Mair, M., Patrick, J. and Steeg, P. S. (2002). Nm23-H1 metastasis suppressor phosphorylation of kinase suppressor of Ras via a histidine protein kinase pathway. *J. Biol. Chem.* **277**, 32389-32399.
Heimann, R. and Hellman, S. (2000). Individual characterisation of the metastatic capacity of human breast carcinoma. *Eur. J. Cancer* **36** 13 Spec No, 1631-1639.
Hippe, H. J., Wolf, N. M., Abu-Taha, I., Mehringer, R., Just, S., Lutz, S., Niroomand, F., Postel, E. H., Katus, H. A., Rottbauer, W. et al. (2009). The interaction of nucleoside diphosphate kinase B with Gbetagamma dimers controls heterotrimeric G protein function. *Proc. Natl. Acad. Sci. USA* **106**, 16269-16274.
Hippe, H. J., Wolf, N. M., Abu-Taha, H. I., Lutz, S., Le Lay, S., Just, S., Rottbauer, W., Katus, H. A. and Wieland, T. (2011). Nucleoside diphosphate kinase B is required for the formation of heterotrimeric G protein containing caveolae. *Naunyn Schmiedebergs Arch. Pharmacol.* **384**, 461-472.
Hofmann, E. R., Milstein, S., Boulton, S. J., Ye, M., Hofmann, J. J., Stergiou, L., Gartner, A., Vidal, M., Hengartner, M. O. (2002). *Caenorhabditis elegans* HUS-1 is a DNA damage checkpoint protein required for genome stability and EGL-1-mediated apoptosis. *Curr. Biol.* **12**, 908-918.
Hurd, D. D. and Kemphues, K. J. (2003). PAR-1 is required for morphogenesis of the Caenorhabditis elegans vulva. *Dev. Biol.* **253**, 54-65.
Igawa, M., Rukstalis, D. B., Tanabe, T. and Chodak, G. W. (1994). High levels of nm23 expression are related to cell proliferation in human prostate cancer. *Cancer Res.* **54**, 1313-1318.
Inoue, T., Sherwood, D. R., Aspöck, G., Butler, J. A., Gupta, B. P., Kirouac, M., Wang, M., Lee, P. Y., Kramer, J. M., Hope, I. et al. (2002). Gene expression markers for Caenorhabditis elegans vulval cells. *Mech. Dev.* **119** Suppl 1, S203-S209.
Kokel, M., Borland, C. Z., DeLong, L., Horvitz, H. R. and Stern, M. J. (1998). clr-1 encodes a receptor tyrosine phosphatase that negatively regulates an FGF receptor signaling pathway in Caenorhabditis elegans. *Genes Dev.* **12**, 1425-1437.
Kolch, W. (2005). Coordinating ERK/MAPK signalling through scaffolds and inhibitors. *Nat. Rev. Mol. Cell Biol.* **6**, 827-837.
Kornfeld, K., Hom, D. B. and Horvitz, H. R. (1995). The ksr-1 gene encodes a novel protein kinase involved in Ras-mediated signaling in C. elegans. *Cell* **83**, 903-913.
Lee, M. Y., Jeong, W. J., Oh, J. W. and Choi, K. Y. (2009). NM23H2 inhibits EGF- and Ras-induced proliferation of NIH3T3 cells by blocking the ERK pathway. *Cancer Lett.* **275**, 221-226.
Mocan, I., Georgescauld, F., Gonin, P., Thoraval, D., Cervoni, L., Giartosio, A., Dabernat-Arnaud, S., Crouzet, M., Lacombe, M. L. and Lascu, I. (2007). Protein phosphorylation corrects the folding defect of the neuroblastoma (S120G) mutant of human nucleoside diphosphate kinase A/Nm23-H1. *Biochem. J.* **403**, 149-156.
Mochizuki, T., Bilitou, A., Waters, C. T., Hussain, K., Zollo, M. and Ohnuma, S. (2009). Xenopus NM23-X4 regulates retinal gliogenesis through interaction with p27Xic1. *Neural Dev.* **4**, 1.
Müller, J., Ory, S., Copeland, T., Piwnica-Worms, H. and Morrison, D. K. (2001). C-TAK1 regulates Ras signaling by phosphorylating the MAPK scaffold, KSR1. *Mol. Cell* **8**, 983-993.
Nicholas, H. R. and Hodgkin, J. (2004). The ERK MAP kinase cascade mediates tail swelling and a protective response to rectal infection in C. elegans. *Curr. Biol.* **14**, 1256-1261.
O'Connell, K. F., Leys, C. M. and White, J. G. (1998). A genetic screen for temperature-sensitive cell-division mutants of Caenorhabditis elegans. *Genetics* **149**, 1303-1321.
Ohmachi, M., Rocheleau, C. E., Church, D., Lambie, E., Schedl, T. and Sundaram, M. V. (2002). C. elegans ksr-1 and ksr-2 have both unique and redundant functions and are required for MPK-1 ERK phosphorylation. *Curr. Biol.* **12**, 427-433.
Rochdi, M. D., Laroche, G., Dupré, E., Giguère, P., Lebel, A., Watier, V., Hamelin, E., Lépine, M. C., Dupuis, G. and Parent, J. L. (2004). Nm23-H2 interacts with a G protein-coupled receptor to regulate its endocytosis through an Rac1-dependent mechanism. *J. Biol. Chem.* **279**, 18981-18989.
Salerno, M., Palmieri, D., Bouadis, A., Halverson, D. and Steeg, P. S. (2005). Nm23-H1 metastasis suppressor expression level influences the binding properties, stability, and function of the kinase suppressor of Ras1 (KSR1) Erk scaffold in breast carcinoma cells. *Mol. Cell. Biol.* **25**, 1379-1388.
Sieburth, D. S., Sundaram, M., Howard, R. M. and Han, M. (1999). A PP2A regulatory subunit positively regulates Ras-mediated signaling during Caenorhabditis elegans vulval induction. *Genes Dev.* **13**, 2562-2569.
Steeg, P. S., Bevilacqua, G., Kopper, L., Thorgeirsson, U. P., Talmadge, J. E., Liotta, L. A. and Sobel, M. E. (1988). Evidence for a novel gene associated with low tumor metastatic potential. *J. Natl. Cancer Inst.* **80**, 200-204.
Steeg, P. S., Palmieri, D., Ouatas, T. and Salerno, M. (2003). Histidine kinases and histidine phosphorylated proteins in mammalian cell biology, signal transduction and cancer. *Cancer Lett.* **190**, 1-12.
Sternberg, P. W. (2005). Vulval development. *WormBook: The Online Review of C. elegans Biology* (ed. The C. elegans Research Community). doi/10.1895/wormbook.1.6.1, http://www.wormbook.org.
Sundaram, M. and Han, M. (1995). The C. elegans ksr-1 gene encodes a novel Raf-related kinase involved in Ras-mediated signal transduction. *Cell* **83**, 889-901.
Sundaram, M., Yochem, J. and Han, M. (1996). A Ras-mediated signal transduction pathway is involved in the control of sex myoblast migration in Caenorhabditis elegans. *Development* **122**, 2823-2833.
Szewczyk, N. J. and Jacobson, L. A. (2003). Activated EGL-15 FGF receptor promotes protein degradation in muscles of Caenorhabditis elegans. *EMBO J.* **22**, 5058-5067.
Takadate, T., Onogawa, T., Fujii, K., Motoi, F., Mikami, S., Fukuda, T., Kihara, M., Suzuki, T., Takemura, T., Minowa, T. et al. (2012). Nm23/nucleoside diphosphate kinase-A as a potent prognostic marker in invasive pancreatic ductal carcinoma identified by proteomic analysis of laser micro-dissected formalin-fixed paraffin-embedded tissue. *Clin. Proteomics* **9**, 8.
Tso, P. H., Wang, Y., Yung, L. Y., Tong, Y., Lee, M. M. and Wong, Y. H. (2013). RGS19 inhibits Ras signaling through Nm23H1/2-mediated phosphorylation of the kinase suppressor of Ras. *Cell. Signal.* **25**, 1064-1074.
Wagner, P. D. and Vu, N. D. (1995). Phosphorylation of ATP-citrate lyase by nucleoside diphosphate kinase. *J. Biol. Chem.* **270**, 21758-21764.
Yochem, J., Sundaram, M. and Han, M. (1997). Ras is required for a limited number of cell fates and not for general proliferation in Caenorhabditis elegans. *Mol. Cell. Biol.* **17**, 2716-2722.
Yoder, J. H., Chong, H., Guan, K. L. and Han, M. (2004). Modulation of KSR activity in Caenorhabditis elegans by Zn ions, PAR-1 kinase and PP2A phosphatase. *EMBO J.* **23**, 111-119.